Journal of Physical and Theoretical Chemistry
of Islamic Azad University of Iran, 14 (3) 187-209: Fall 2017
(J. Phys. Theor. Chem. IAU Iran)
ISSN 1735-2126

Electronic Structure, Biological Activity, Natural Bonding Orbital (NBO) and Non-Linear Optical Properties (NLO) of Poly-Functions Thiazolo [3,2-a]Pyridine Derivatives. DFT Approach

Shimaa Abdel Halim[1,*] and H. Moustafa[2]

[1] Department of Chemistry, Faculty of Education, Ain Shams University, Roxy 11711, Cairo, Egypt
[2] Department of Chemistry, Faculty of Science, Cairo University, Giza, Egypt

Received December 2017; Accepted March 2018

ABSTRACT

The optimized structures of studied compounds **23-28** are non planner with the two phenyl at C_3 and C_9 are out of the molecular plane of thiazolo[3,2-a]pyridine as indicated from a dihedral angles of 71^0 and 116^0 respectively, using DFT-B3LYP method with 6-311G(d,p) as basis set. The natural bonding orbital (NBO) analysis of the parent molecule **23** have been analyzed in terms of the hybridization of each bond, natural charges, bonding and antibonding orbital's, and second order perturbation energy ($E^{(2)}$). The calculated E_{HOMO} and E_{LUMO} energies of the studied compounds can be used to explain the extent of charge transfer in the molecule and to calculate the global properties; the chemical hardness (η), global softness (S), electrophilicity (ω), and electronegativity (χ). The effect of substituent's of different strengths on the geometry, energetic and nonlinear optical properties are analyzed and discussed. The NLO parameters: static dipole moment (μ), polarizability (α), anisotropy polarizability ($\Delta\alpha$), and first order hyperpolarizability (β_{tot}), of the studied compounds have been calculated at the same level of theory and compared with the proto type Para-Nitro-Aniline (PNA). The results of (β_{tot}) promising electrical properties. The 3D plots of the molecular electrostatic potential (MEP) for some selected compounds were investigated and describing the electrophilic and nucleophilic sites. The biological activity of the studied compounds was tested against gram positive, gram negative and Fungi. A correlation between energetic, global properties and biological activity were investigated and discussed.

Keywords: DFT calculations; substituent effect**;** thiazolo[3,2-a]pyridine; biological activity; NLO and NBO analysis

1. INTRODUCTION

Thiazolo[3,2-a]pyridine, containing two fused heterocyclic rings have a wide range of biological activities such as inhibiting beta-amyloid production, [1] potent CDK2-Cyclin A inhibitor, [2] a-glucosidase inhibitor, [3] potential uterus stimulant, [4]coronary dilator, antihypertensive and muscle relaxant activities, [5] antibacterial and antifungal activities [6]. Thiazolo[3,2-a]pyridine derivatives are found to exhibit a broad spectrum of potent anticancer activity and are useful for chemotherapy of various cancers, such as leukemia, lung cancer, and melanoma [7]. Thiazolo[3,2-a]pyridine derivatives have become synthetic targets for many organic and medicinal chemistry

*Corresponding author: Shimaaquantum@ymail.com

[8,9]. The antifungal and antibacterial activities of the 5-amino-2-phenylmethylidene-7-phenyl-6,8-dicyano-3-oxo-2,3-dihydro-7H-thiazolo[3,2-a]pyridines **(parent molecule23**) were measured and synthesized experimentally [10]. The results indicate that P-OCH3, P-F and P-Br substituent'saremore active than the P-Cl and P-CH3. Also; thiazolo[3,2-a]pyridinehave antioxidant and cytotoxic activities [4].

The NLO properties depend on the extent of charge transfer (CT) interaction across the conjugative paths and the electron transfer ability of an aromatic ring and on its ionization potential (IP) and electron affinity (EA) [11, 12]. Linear polarizability $\langle \Delta\alpha \rangle$ and first order hyperpolarizability $\langle \beta \rangle$ are required for the rational design of optimized materials for photonic devices such as electro optic modulators and all-optical switches [13, 14]. Natural bond orbital (NBO) analysis wasoriginatedas a technique for studying hybridization and covalence effects in polyatomic wave functions. The work of Foster and Weinhold [15] was extended by Reed et al., [16] who employed NBO analysis that exhibited particularly H-bonded and other strongly bound van-der Waals complexes. In our previous work [17] the electronic absorption spectra of the studied compounds are investigated experimentally in Dioxane and DMF; and theoretically in gas phase, Dioxane and DMF using TD-DFT-B3LYP/6-311G (d, p).Theoretical calculations of the vertical excitations reproduce the experimental spectra, indicating a good agreement between theory and experiment. The effect of substituent's of different strengths on the observed spectra was analyzed. In the literature there is no systematic study of the electronic structure, substituent effect and bonding characteristics of the studied compounds. Therefore, our contribution here is to shed more light on the geometric structure and ground state properties of the 5-amino-2-phenylmethylidene-7-phenyl-6,8-dicyano-3-oxo-2,3-dihydro-7H-thiazolo[3,2-a]pyridines derivatives using DFT-B3LYP and a basis set 6-311G (d,p). Natural bonding orbital's (NBO) and nonlinear optical (NLO) parameterizes are investigating to identify and characterize the forces that govern the structure-activity and the optical properties of the studied compounds. The biological activity of the studied compounds was tested against gram positive, gram negative and Fungi. A correlation between energetic, global properties and biological activity were investigated and discussed.

The compounds studied in this work are shown below:

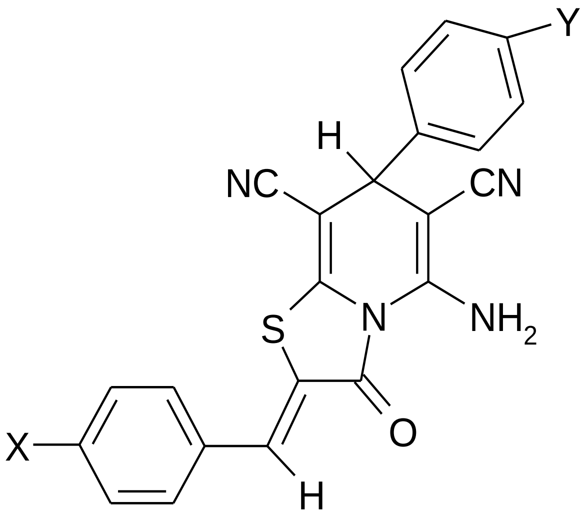

Compounds	X	Y
23	H	H
24	CH_3	CH_3
25	OCH_3	OCH_3
26	NO_2	NO_2
27	Cl	Cl
28	Br	Br

2. COMPUTATIONAL METHOD

Calculations have been performed using Khon-Sham' s DFT method subjected to the gradient-corrected hybrid density functional B3LYP method [18]. This function is a combination of the Becke' s three parameters non-local exchange potential with the non-local correlation functional of Lee et al [19].For each structure, a full geometry optimization was performed using this function[19] and the 6-311G (p,d) bases set [20] as implemented by Gaussian 09 package [21]. All geometries were visualized either using GaussView 5.0.9 [22] or chemcraft 1.6 [23] software packages. No symmetry constrains were applied during the geometry optimization. Also, the total static dipole moment (μ), $\langle\Delta\alpha\rangle$, $\langle\beta\rangle$ and $\langle\gamma\rangle$, values were calculated by using the following equations [24-26]:

$$\mu = (\mu^2_x + \mu^2_y + \mu^2_z)^{1/2},$$

$$\langle\alpha\rangle = 1/3(\alpha_{xx} + \alpha_{yy} + \alpha_{zz}),$$

$$\Delta\alpha = \left((\alpha_{xx} - \alpha_{yy})^2 + (\alpha_{yy} - \alpha_{zz})^2 + (\alpha_{zz} - \alpha_{xx})^2 / 2\right)^{1/2},$$

$$\langle\beta\rangle = (\beta^2_x + \beta^2_y + \beta^2_z)^{1/2},$$

where

$$\beta_x = \beta_{xxx} + \beta_{xyy} + \beta_{xzz},$$

$$\beta_y = \beta_{yyy} + \beta_{xxy} + \beta_{yzz},$$

$$\beta_z = \beta_{zzz} + \beta_{xxz} + \beta_{yyz}.,$$

By using HOMO and LUMO energy values, electronegativity, and chemical hardness can be calculated as follows: $\chi = (I + A)/2$ (electronegativity), $\eta = (I - A)/2$ (chemical hardness), $S = 1/2\eta$ (global softness), $\omega = \mu^2/ 2\eta$ (electrophilicity) where I and A are ionization potential and electron affinity, and $I = -E_{HOMO}$ and $A = -E_{LUMO}$, respectively [27, 28]. The population analysis has been performed [29] at B3LYP/6-311G (d,p) level of theory using natural bond orbital (NBO) under Gaussian 09programpackage. The second-order Fock matrix was used to evaluate the donor-acceptor interactions in the NBO basis [30]. For eachdonor(i) and acceptor (j), the stabilization energy $E^{(2)}$ associated with the delocalization $i \rightarrow j$ is estimated as

$$E^{(2)} = \Delta E_{ij} = q\left(F(ij)^2 / \varepsilon_j - \varepsilon'_i\right),$$

where $q_i$is the donor orbital occupancy, ε_i and $\varepsilon_j$are diagonalelements and $(ij)$is the off-diagonal NBO Fock matrix element. The conversion factors for α, β, and HOMO andLUMO energies in atomic and cgs units: 1 atomic unit(a.u.) = 0.1482 $\times 10^{-24}$ electrostatic unit (esu) for polarizability; 1 a.u. = 8.6393$\times 10^{-33}$esu for first hyperpolarizability;1 a.u. = 27.2116 eV (electron volt) for HOMO and LUMOenergies.

3. RESULTS AND DISCUSSION

3.1.1. Partitioning of the 5-amino-2-phenylmethylidene-7-phenyl-6,8-dicyano-3-oxo-2,3-dihydro-7H-thiazolo[3,2-a]pyridines (23)

Due to the complexity of the parent molecule and the presence of multi-functions attached to the fused ring e.g. two cyano groups at C_2 and C_4, amino groupat C_1, carbonyl group at C_{10}, the phenyl ring at C_3, phenyl methylidene ring at C_9 and two hetero atoms; nitrogen, and sulfur in the fused ring. The parent compound **23** is portioned into twenty two subsystems(**1-22**) as presented in scheme 1. This partitioning of the parent compound **23** is of course, artificial and has only been assumed to enable the predication of the force that governs the electronic properties, biological activity and bonding characteristics of the studied molecule.

To achieve this goal, we start by establishing a good ground state properties and natural bonding orbital (NBO) for each subsystem. The total energy (E_T), energy of highest occupied molecular orbital (E_{HOMO}), energy of lowest unoccupied molecular orbital (E_{LUMO}), energy gap (E_g) and dipole moment (μ) of all subsystems are presented in Table 1. The optimized structure of the parent **23** and its subsystems **1-22**, numbering system, HOMO and LUMO-charge density maps and the vector of dipole moment using B3LYB/6-311G (d,p) are presented in Figures1 and 2. From data in Table 1 and Figures1 and 2;

The subsystems **1-7** (single substituent function), the calculated E_{gap} are greater (less reactive) than the parent **23** by about 1.04 eV (≈ 24 kcal/mol), while the subsystems **8-22** (double substituent functions), the computed E_{gap} are greater (less reactive) than the parent **23** by 0.56eV (≈ 13 kcal/mol). Therefore, all functions must be attached to the fused thiazolo[3,2-a]pyridine the parent molecule leading to its reactivity. From the computed dipole moment, it's found that the presence of two cyano groups at C_2 and C_4 and phenyl methylidene group at C_9 (c.f. Figure. 1) are responsible for the polarity of the compound **23** (c.f. Table 1).

Table 1. Total energy, energy of HOMO and LUMO, energy gap and dipole moment of the parent (**23**) and its subsystems (**1-22**) computed at the B3LYP/6- 311G(d,P) level of theory

Compounds	E_T (au)	E_{HOMO} (eV)	E_{LUMO} (eV)	E_{gap} (eV)	μ (Debye)
1	-723.949595	-4.548656	-0.091936	4.45672	1.8877
2	-994.916796	-4.786928	-0.716176	4.070168	1.6622
3	-955.055262	-4.703696	-0.542096	4.1616	2.0519
4	-799.236728	-5.783808	-0.60248	5.181328	1.9295
5	-779.321530	-4.482288	-0.0612	4.421088	2.7347
6	-816.218900	-5.236	-1.46744	3.76856	4.7792
7	-816.223066	-5.261568	-1.201696	4.059872	6.9156
8	-1068.98575	-4.9300000	-1.643696	3.286304	2.2774
9	-1050.28910	-4.739056	-0.63512	4.103936	2.3256
10	-1226.02211	-4.824192	-0.7684	4.055792	2.0078
11	-1087.18743	-5.04016	-1.285744	3.754416	5.6185
12	-1087.18847	-5.008064	-1.145936	3.862128	6.8341
13	-854.605930	-5.198736	-0.532576	4.66616	0.7364
14	-891.501881	-6.346032	-1.886048	4.459984	4.9653
15	-891.504394	-6.370784	-1.592288	4.778496	3.0937
16	-1030.34116	-5.888256	-0.829872	5.058384	1.7209
17	-1010.42696	-4.624000	-0.385696	4.238304	2.8772
18	-871.596798	-5.178336	-1.099152	4.079184	4.7852
19	-871.595355	-5.18704	-0.97376	4.21328	7.6519
20	-908.487494	-5.859696	-2.243728	3.615968	6.7079
21	-1047.32310	-5.320592	-1.50144	3.819152	4.6964
22	-1047.32684	-5.337728	-1.284384	4.053344	6.6833
23 (parent)	-1539.9973	-6.28021	-2.82499	3.45522	6.1794

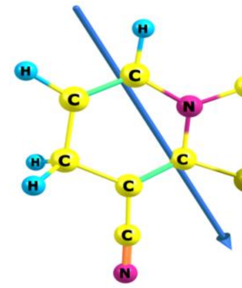

1

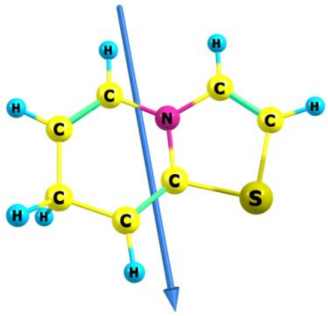

7

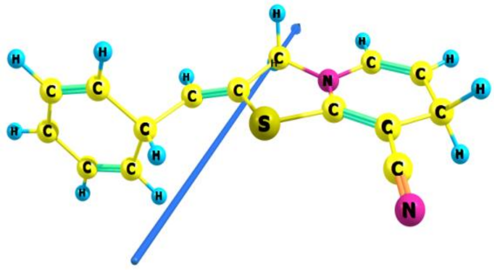

12

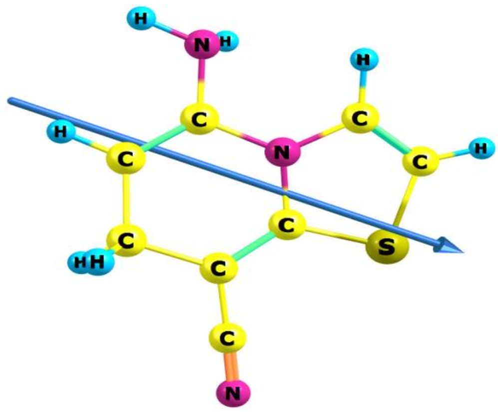

19

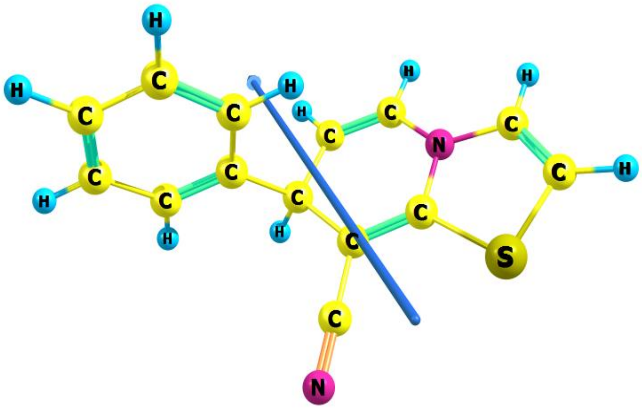

22

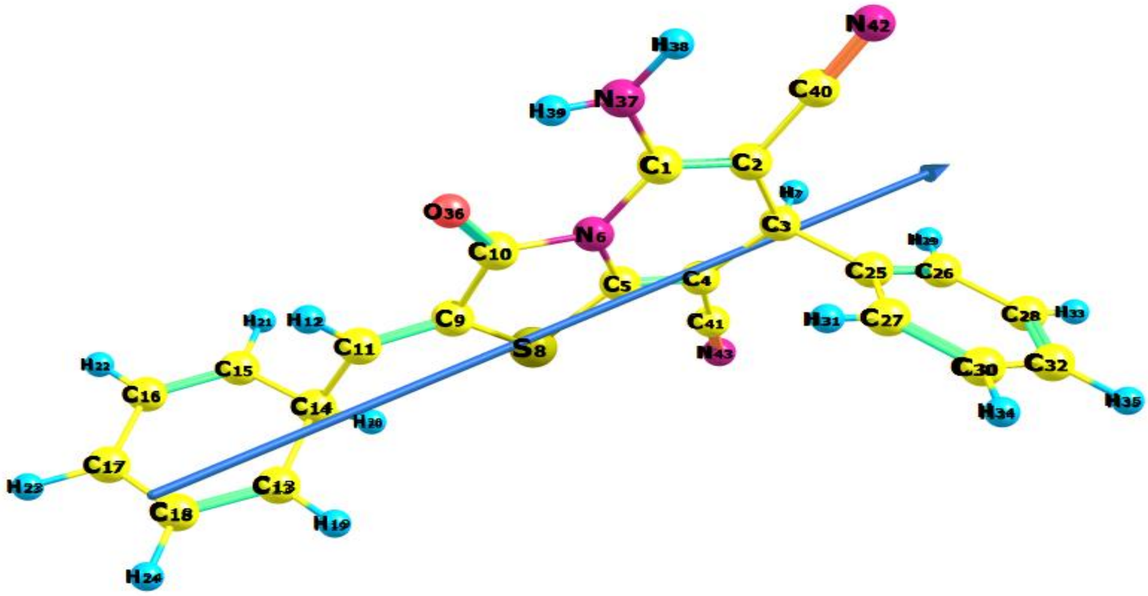

23

Fig. 1. Optimized geometry, vector of the dipole moment and numbering system, for compound **23** andits subsystems **(1, 7, 12, 19, and 22)** at B3LYP/6-311G (d, p).

compound	E_g	HOMO	LUMO
1	4.4567eV	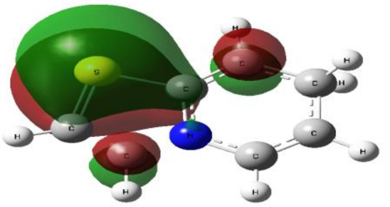	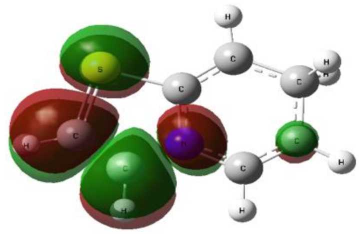
7	4.0599eV	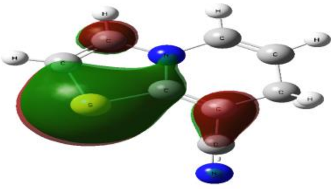	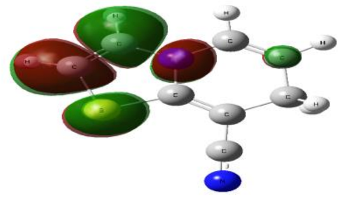
12	3.8621eV	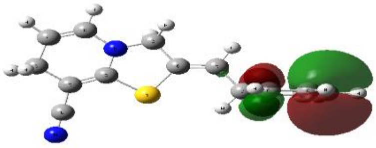	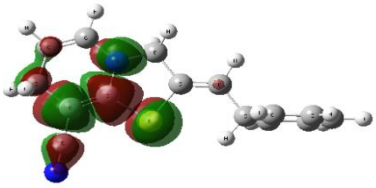
19	4.2132 eV	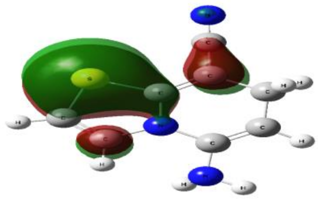	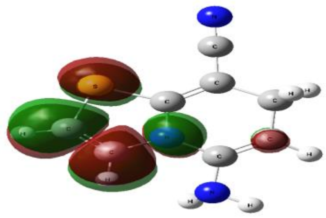
22	4.0533eV	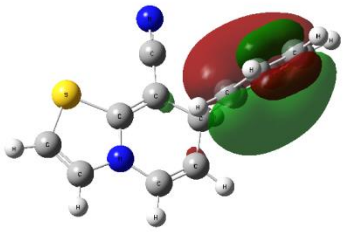	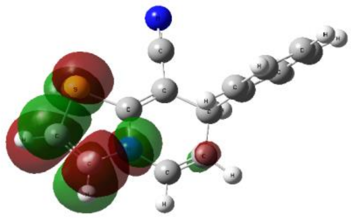
23	3.4552eV	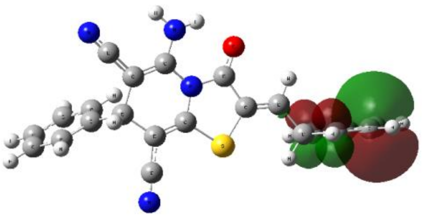	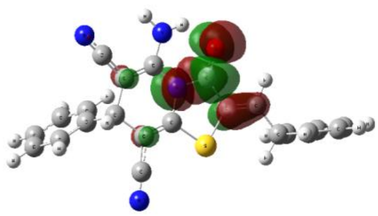

Fig. 2. HOMO, LUMO and energy gap of compound **23** andits subsystems **(1, 7, 12, 19, and 22).**

The optimized geometric parameters (bond lengths, bond angles and dihedral angles) of the parent molecule **23** and some of its effective subsystems 1**, 7, 12, 19,** and **22** using B3LYP/6-311G (d,p) method are listed in Table 2.

The optimized bond lengths and bond angles are compared with the available X-ray experimental data [31–33]. The observed bond lengths of C_1-C_2 and C_3-C_4in pyridine ring are 1.380Å and 1.522Å respectively, while the theoretical values are1.335Å and 1.515Å respectively. For C-S bonds (C_5-S_8 and S_8-C_9), the calculated values are greater than the experimental values by 0.065Å and 0.025Å respectively. The calculated C-N bond in thiazolo [3,2-a]pyridine ring **1**, value is over estimated than that of the experimental value (c.f. Table2). There is a great agreement between the calculated bond lengths of the parent **23** and the experimental values indicating the power of the method used. For subsystem **1,** the calculated bond angles <C4C5S8 (128.4°) and <N6C10C9 (114.6°) are overestimated than the experimental values, whereas, the calculated bond angles <C5N6C1 (118.5°) and <N6C5S8 (108.5°) are underestimated than the experimental values (c.f. Table 2). The effect of different substituent's in the selected subsystems 7**, 12, 19,** and **22** are listed in Table 2. There are disagreement between the calculated bond angle and the experimental values which may be attributed to that the calculation were carried out in the gas phase and the experimental measured in the solid state. All subsystems of the parent molecule **23** are planner except the subsystems **12, 19** and **22** are non-planner as indicating from the calculated dihedral angles (c.f. Table 2).

Table 2. Selected experimental and theoretical bond lengths, bond angles, dihedral angles and natural charge for the parent (**23**) and some of its selected subsystems (**1, 7, 12 , 19 and 22**) computed at the B3LYP/6-311G(d,p) level of theory.

Parameters	**EXP.[31-33]**	**1**	**7**	**12**	**19**	**22**	**23**
Bond lengths (Å)							
C_1–C_2	1.380(4)	1.335	1.332	1.334	1.339	1.333	1.370
C_3–C_4	1.521(4)	1.515	1.527	1.527	1.524	1.533	1.521
C_5–N_6	1.341(4)	1.408	1.388	1.378	1.391	1.387	1.403
C_1–N_6	1.387(3)	1.397	1.405	1.402	1.416	1.403	1.421
C_5–S_8	1.722(3)	1.778	1.767	1.773	1.768	1.768	1.767
S_8–C_9	1.753(2)	1.787	1.770	1.788	1.769	1.769	1.773
C_9–C_{10}	1.399(3)	1.338	1.338	1.510	1.338	1.338	1.483
C_{10}–N_6	1.341(4)	1.388	1.391	1.451	1.395	1.392	1.407
Bond Angles (^{0})							
<N_6-C_1-C_2	123.9(2)	122.01	119.32	121.70	120.04	121.63	119.35
<C_1-C_2-C_3	120.0(3)	123.45	123.73	122.96	123.55	124.12	124.96
<C_2-C_3-C_4	109.3(2)	111.07	109.68	110.75	110.52	109.81	109.75
<C_3-C_4-C_5	120.0(3)	121.84	111.16	121.21	120.14	121.49	122.28
<C_4-C_5-S_8	120.35(2)	128.42	127.88	125.49	127.80	127.85	124.75
<C_5-N_6-C_1	123.9(2)	118.52	119.44	118.53	119.34	119.21	119.08
<N_6-C_5-S_8	115.80(18)	108.48	109.38	111.34	109.53	109.43	111.85
<N_6-C_{10}-C_9	110.6(2)	114.62	114.00	106.21	113.88	113.93	110.15
<S_8-C_9-C_{10}	109.55(18)	111.66	111.63	109.24	111.91	111.71	111.33
<C_9-S_8-C_5	88.96(11)	90.570	90.481	91.441	90.371	91.431	91.051
<N_6-C_1-C_{10}	117.6	126.81	126.05	122.11	126.03	126.09	125.30

Table 2. Continued

Dihedral Angles (^{0})						
$<C_1C_2C_3C_4$	-0.037	-0.032	-7.645	-18.471	-9.845	-9.294
$<C_3C_4C_5N_6$	0.002	-0.011	-0.149	-5.482	-4.449	-3.752
$<C_4C_5N_6C_1$	-0.042	-0.019	-8.009	-10.402	-3.954	-5.977
$<C_4C_5S_8H_{10}$	0.022	-0.002	1.840	-3.003	-2.925	-2.641
$<N_6C_5\ S_8C_9$	0.008	-0.003	2.876	2.283	-0.291	-2.024
$<S_8C_9C_{10}N_6$	0.005	0.000	25.35	-0.510	0.058	0.768
$<H_{14}C_{10}N_6C_1$	0.071	0.028	-62.79	11.332	5.287	5.376
$<S_8C_9C_{11}C_{14}$			0.625	-------	------	-0.470
$<S_8C_9C_{10}C_{11}$			-179.1	-------	------	179.72
$<C_5N_6C_1N_{37}$				-170.63	------	169.82
$<C_3C_4C_{25}C_{27}$					63.69	-71.47
Natural Charge						
C3	-0.4537	-0.3991	-0.4006	-0.3890	-0.2493	-0.1962
C4	-0.2693	-0.2427	-0.2325	-0.2414	-0.2425	-0.2478
N6	-0.4615	-0.4284	-0.4609	-0.4405	-0.4247	-0.4499
S8	0.5217	0.3638	0.3308	0.3643	0.3675	0.3687
C9	-0.4426	-0.3901	-0.1809	-0.3883	-0.3888	-0.2540
N17		-0.3560	-0.3503	-0.3592	-0.3518	-0.3535
N15				-0.8116		-0.7640

3.1.2. Natural charge analysis

Natural charge analysis isperformed on the electronic structure sclearly describes the distribution of electrons in various sub shells of their atomic orbital's [34]. The natural charges and natural populations for subsystems **1, 7, 12, 19, 22** and the parent **23** calculatedat B3LYP/6-311G (d, p) level of theory is also presented in (Table 2). For the subsystem **1**, the most electronegative charges are accumulated on C3, N6 and C9. According to an electrostatic point of view of the molecule, these electronegative atoms have a tendency to donate electrons. Whereas, the most electropositive atoms such as; S8 have a tendency to accept electrons in Table 2. The natural charge plot with B3LYP/6-311G (d,p) method are shown in Figure 5. It is noted that from Figure 5, the strong negative and positive partial charges on the skeletal atoms of the parent (especially O_{36}, S_8, C_1, C_2, N_6, N_{37}, N_{43}, C_{10}, C_4, C_9, $C_{14,}$ C_{18}, $C_{40,}$ H_{38}, H_{39}) increases with increasing Hammett constant of substituent groups. These distributions of partial charges on the skeletal atoms show that the electrostatic repulsion or attraction between atoms can give a significant contribution to the intra- and intermolecular interaction.

3.1.3. Natural bonding orbital (NBO) analysis

The NBO analysis provides an efficient method for studying intra-and intermolecular bonding as well as it acts as a convenient basis for investigating charge transfer or conjugative interactions in molecular systems. Table 3 presents the second order perturbation energies between high energy Lewis NBOs (donors) and low energy non-Lewis NBOs (acceptors) of the subsystems **1, 7, 12, 19,** and **22** (the high value of E^2 indicates stronger interactions).

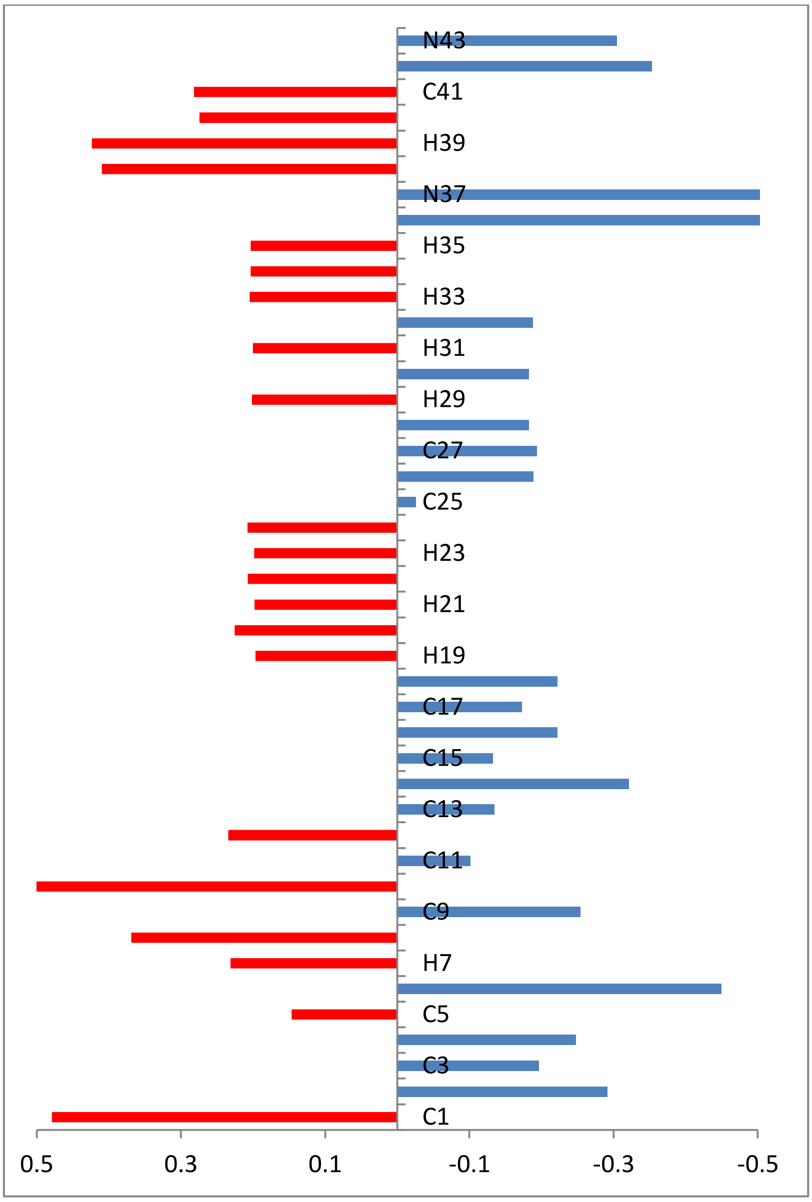

Atomic charge distribution

Negative Charge value   Positive Charge value   For numbering system, see **Fig.1 or Fig.3**

Fig. 5. Atomic charge distribution (au) for 5-amino-2-phenylmethylidene-7-phenyl-6,8-dicyano-3-oxo-2,3-dihydro-7H-thiazolo[3,2-a]pyridine **(23)** at B3LYP/6-311G(d,p) basis set.

The charge density maps of HOMO and LUMO for the subsystems **1, 7, 12, 19,** and **22** subsystems are presented in Figure 2. The values of $E^2$for subsystem **1**, indicate that there is a strong hyper conjugative interactions between LP(2)S8 → π*C9-C10, and LP(1)N6 → π*(C4-C5) as revealed by their values of 69.80 and 36.09 kcal/mol, respectively (c.f. Table 3). The NBO bond polarization and hybridization change of subsystem **1** are collected in (Table 3) indicate that C3 and C4 in the bond hybrid of the σC3–C4 has $sp^{3.09}$ hybrid orbital. The donor-acceptor transition represented by [σC3-C4→σ*C5-S8] has a CT character with a value of 5.99 kcal/mol as shown below:

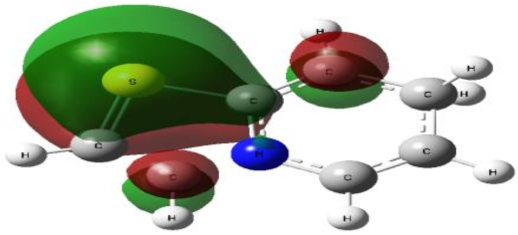

HOMO

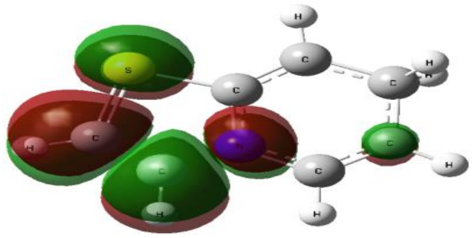

LUMO

Intermolecular hyper conjugative interactions of the subsystems **1, 7, 12, 19,** and **22** (c.f. Table 3 and Figure. 2) are formed by the orbital overlap between bonding and antibonding orbital's which results in intermolecular charge transfer (CT) causing stabilization of the molecular system. These interactions are observed as an increase in electron density (ED) in the antibonding orbital's that weakness the bond character. For example, the π*(C4–C5) in the subsystem **7**, distributes charge density to [LP(1)N6 and LP (2)S8] with stabilization energy 38.24, 22.92 kcal/mol respectively. The values of E^2andthe orbital overlap between bonding and antibondingorbital'sfor the subsystems **12, 19,** and **22**are listedin Table 3.

Table 3. Second Order Perturbation Interaction Energy Values Computed in the NBO Basis, Occupancy of natural orbital's (NBOs) and hybrids for the parent **23** and some of its selected subsystems (**1, 7, 12 , 19 and 22**) by B3LYP/6-311G (d,p)

Compound	Donor	Acceptor	$E^{(2)a}$(kcal/mol)	Donor Lewis-type (NBOs)	Occupancy	Hybrid
1	σC3-C4	σ*C5-S8	5.99	C3-C4	1.96588	$sp^{3.09}$
	πC3-H16	π*C4-C5	6.89	C3-H16	1.95099	$sp^{4.39}$
	LP (1) N6	π*C4-C5	36.09	LP (1) N6	1.61650	$p^{1.00}$
	LP(2) S8	π*C9- C10	69.80	LP(2) S8	1.51039	$p^{1.00}$
7	σC2-H9	σ*C1-N6	7.48	C2-H9	1.97201	$sp^{2.51}$
	σC3-C4	σ*C5-S8	6.68	C3-C4	1.95905	$sp^{2.47}$
	πC4-C5	π*C41-N43	15.07	C4-C5	1.88177	$p^{1.00}$
	LP (1) N6	π*C4-C5	38.24	LP (1) N6	1.61292	$p^{1.00}$
	LP(2) S8	π*C4-C5	22.92	LP(2) S8	1.73670	$p^{1.00}$
	LP (1) N43	RY* C41	10.22	LP (1) N43	1.96859	$sp^{0.51}$
	LP (1) N43	σ*C4-C41	13.01	C4-C5	0.34997	$p^{1.00}$
	π*C4-C5	π*C41-N43	60.28			
12	πC4-C5	π*C41-N43	7.93	C4-C5	0.93714	$p^{1.00}$
	σC11-H12	σ*S8- C9	5.22	C11-H12	0.98174	$sp^{2.69}$
	LP (1) N6	π*C4-C5	18.09	LP (1) N6	0.85059	$p^{1.00}$
	LP(2) S8	π*C4-C5	11.06	LP(2) S8	0.88154	$p^{1.00}$
	LP (1) C17	π*C15-C16	36.83	LP (1) C17	0.73498	$p^{1.00}$
19	σC2-H8	σ*C1-N6	8.20	σC2-H8	1.97130	$sp^{2.53}$
	πC4-C5	π*C41-N43	15.68	πC4-C5	1.87400	$p^{1.00}$
	LP (1) N6	π*C4-C5	36.74	LP (1) N6	1.62176	$p^{1.00}$
	LP(2) S8	π*C4-C5	22.67	LP(2) S8	1.73490	$p^{1.00}$
	LP (1) N37	π*C1- C2	14.53	LP (1) N37	1.89024	$p^{1.00}$
	LP (1) N43	σ*C4- C41	13.20	LP (1) N43	1.96876	$sp^{0.41}$

Table 3. Continued

22	σC2-H8	σ*C1-N6	7.27	C2-H8	1.97194	$sp^{2.51}$
	σC3-C4	σ*C5-S8	6.41	C3-C4	1.94977	$sp^{2.75}$
	πC4-C5	π*C41-N43	14.81	C4-C5	1.88010	$p^{1.00}$
	πC25-C26	π*C28-C32	20.59	C25-C26	1.66206	$p^{1.00}$
	πC27-C30	π*C25-C26	21.02	C27-C30	1.66572	$p^{1.00}$
	LP (1) N6	π*C4-C5	38.85	LP (1) N6	1.60845	$p^{1.00}$
	LP (2) S8	π*C4-C5	22.90	LP (2) S8	1.73435	$p^{1.00}$
	LP (1) N43	σ*C4- C41	13.28	LP (1) N43	1.96828	$sp^{0.47}$
	π*C4-C5	π*C41-N43	73.36	C4-C5	0.35825	$p^{1.00}$
23	σC1-C2	σ*C40-N42	16.47	C5-N6	0.41312	$sp^{2.51}$
	πC28-C32	π*C25-C26	12.53	C13-C18	0.13944	$p^{1.00}$
	LP (1) C4	π*C5-N6	334.88	C25-C26	0.17550	$p^{1.00}$
	LP (1) C4	π*C41-N43	35.64	C1-C2	0.88101	$p^{1.00}$
	LP(2) S8	σ*C5- N6	15.84	C10-O36	0.17884	$sp^{0.47}$
	LP (1) N6	π*C10-O36	24.72	C28-C32	0.82919	$p^{1.00}$
	LP (1) C17	σ*C13-C18	37.01	LP(2) S8	0.87620	$sp^{0.47}$
	LP (1) N37	π*C1-C2	24.43	LP (1) C17	0.73023	$p^{1.00}$
	π*C1-C2	π*C40-N42	79.39	LP (1) C4	0.56005	$p^{1.00}$
	π*C10-O36	π*C9-C11	24.63	LP (1) N37	0.86742	$p^{1.00}$
	LP (2)O36	π*N6-C10	13.52			
	LP(1) N43	RY*C41	11.14			

[a] $E^{(2)}$ means energy of hyper conjugative interactions (stabilization energy).
$LP_{(n)}$ is a valence lone pair orbital (n) on atom.

3.2. Substituent effect on molecular geometry

The effect of substituent of different electron donating / withdrawing power at C3-phX and C9-phY on the geometrical parameters (bond lengths, bond angles and dihedral angles) of the studied compounds **23-28**, is listed in Table 4 and 5. The computed bond lengths and bond angles are compared with the available experimental data [31–33]. The global energy minimum obtained by the DFT-B3LYP/6-311G (d,p) and the vector of the dipole moment are presented in Figure 3. The calculated bond lengths C1-C2, C2-C3, C3-C4 and C4-C5 of the fused thiazolo-pyridine are overestimated than the experimental values by 1%, whereas, the computed C1-N6 and C5-N6 bond lengths are overestimated than the experimental values by 4%. At the same time, the computed C5-S and C9-S bond lengths are overestimated than the experimental values by 2.5%. The small difference between calculated and observed bond lengths indicates the power of the method used in calculation. No significant change in the calculated bond angles of the studied compounds **23-28** on comparing with the experimental values. The small difference between calculated and observed angles may be attributed to that the calculations were carried out in gas phase and observed in solid state. All the studied compounds **23-28** are non-planner as reflected from their dihedral angles. In the parent compound **23**, the C3-ph and C9-ph moieties are out of the molecular plane of the fused thiazolo-pyridine by dihedral angles equal 70^o and 116^o respectively. Upon substitution no significant change in the dihedral angles of the C3-ph-X while the dihedral angles of C9-ph-Y moiety decreased and become nearly planner (c.f. Table 4 and 5).

Table 4. Selected experimental and theoretical bond lengths, and bond angles for the the studied compounds (23-28) computed at the B3LYP/6-311G(d,P) level of theory

Parameters	**EXP.[31-33]**	**23**	**24**	**25**	**26**	**27**	**28**
Bond lengths (Å)							
C1 - C2	1.380(4)	1.370	1.370	1.370	1.371	1.371	1.370
C2 – C3	1.521(4)	1.517	1.518	1.518	1.516	1.517	1.518
C4 – C5	1.371(4)	1.348	1.349	1.349	1.348	1.349	1.349
C5 – N6	1.341(4)	1.403	1.399	1.399	1.399	1.399	1.399
C1 - N6	1.387(3)	1.421	1.420	1.419	1.421	1.421	1.420
C5 – S8	1.722(3)	1.767	1.766	1.766	1.767	1.766	1.766
S8 – C9	1.753(2)	1.773	1.766	1.768	1.761	1.765	1.766
C9 – C10	1.399(3)	1.483	1.478	1.475	1.485	1.480	1.480
C10 - N6	1.341(4)	1.406	1.409	1.411	1.406	1.409	1.409
C1 – N37	1.335(3)	1.354	1.354	1.355	1.352	1.352	1.353
C2 – C40	1.389(4)	1.414	1.414	1.414	1.414	1.414	1.414
C40 – N42	1.290(3)	1.159	1.159	1.159	1.159	1.159	1.159
C3 – C25	1.524(4)	1.533	1.531	1.531	1.534	1.532	1.532
C4 – C41	1.389(4)	1.419	1.419	1.418	1.419	1.419	1.419
C41 – N43	1.290(3)	1.157	1.157	1.157	1.157	1.157	1.157
C9 – C11	1.371(4)	1.338	1.351	1.353	1.350	1.351	1.351
C11 – C14	1.512(3)	1.515	1.449	1.446	1.452	1.450	1.450
Bond Angles (0)							
<N6-C1-C2	123.9(2)	119.35	119.32	119.36	119.26	119.31	119.27
<C1-C2-C3	120.0(3)	124.96	124.96	124.99	124.98	124.99	124.95
<C2-C3-C4	109.3(2)	109.75	109.68	109.59	109.90	109.80	109.80
<C3-C4-C5	120.0(3)	122.28	122.14	122.13	122.03	122.11	122.07
<C5-N6-C1	123.9(2)	119.08	119.07	119.04	119.08	119.08	119.08
<N6-C5-S8	115.80(18)	111.85	111.58	111.53	111.66	111.63	111.62
<N6-C10-C9	110.6(2)	110.15	110.40	110.39	110.35	110.38	110.36
<C10-C9-S8	109.55(18)	111.33	111.11	111.15	111.07	111.09	111.10
<C9-S8-C5	88.96(11)	91.050	91.415	91.408	91.462	91.431	91.438
<C1-N37H39	117.6	118.88	118.80	118.59	119.43	119.15	119.00
<N6-C1-N37	121.0(2)	116.20	116.26	116.20	116.29	116.28	116.28
<C2-C1-N37	124.6(2)	124.38	124.35	124.37	124.40	124.36	124.38
<C2-C40-N42	179.7	178.10	178.10	178.04	178.16	178.17	178.29
<C3-C2-C40	116.6(3)	117.99	117.95	117.99	117.92	117.91	117.90
<C2-C3-C25	110.9(3)	113.28	113.03	113.47	113.43	113.29	113.00
<C25-C3-C4	110.9(3)	111.02	111.27	111.13	110.57	110.93	111.17
<C4-C3-H7	109.5	107.47	107.51	107.44	107.47	107.46	107.53
<C10-N6-C1	124.8(3)	125.30	125.44	125.46	125.44	125.44	125.44
<C11-C9-S8	130.8(2)	126.87	129.31	129.12	129.71	129.45	129.48
<C11-C9-C10	120.0(3)	121.80	119.59	119.73	119.21	119.45	119.42
<C9-C11-H12	117.6	116.64	112.78	112.65	112.98	112.83	112.81
<C9-C11-C14	120.0(3)	126.42	131.74	131.89	131.45	131.70	131.71
<C14-C11H12	117.6	116.94	115.47	115.45	115.56	115.47	115.47

Table 5. Dihedral Angles (^{0}) and Natural Charge for the studied compounds **(23-28)** computed at the B3LYP/6-311G(d,P) level of theory

Parameters	23	24	25	26	27	28
Dihedral Angles (^{0})						
$<C_1C_2C_{40}N_{42}$	-9.036	-10.119	-7.491	-5.923	-9.013	-10.742
$<C_{40}C_2C_1N_{37}$	1.582	1.395	1.791	0.972	1.078	1.377
$<C_2C_1N_{37}H_{39}$	-167.82	-168.33	-167.38	-170.29	-169.61	-168.67
$<C_{40}C_2C_3H_7$	-53.040	-52.954	-53.013	-53.433	-53.486	-53.016
$<C_4C_3C_{25}C_{27}$	-71.47	-63.361	-63.154	-62.575	-62.634	-63.275
$<C_3C_4C_{41}N_{43}$	-70.150	-60.571	-62.055	-65.479	-66.196	-69.928
$<C_1N_6C_{10}O_{36}$	-5.376	-5.172	-5.276	-4.670	-4.903	-5.146
$<C_{10}C_9C_{11}H_{12}$	-0.436	-0.226	-0.185	0.036	-0.134	-0.211
$<C_9C_{11}C_{14}C_{15}$	-116.41	-177.35	-178.18	-175.42	-176.87	-179.31
$<C_9C_{11}C_{14}H_{20}$	1.37	0.593	0.499	0.961	0.753	0.208
$<C_9C_{11}C_{14}H_{12}$	-179.64	-179.69	-178.51	-179.34	-179.52	-179.81
$<C_5S_8C_9C_{11}$	-179.59	-179.73	-179.41	-179.79	-179.71	-179.24
Natural Charge						
C1	0.4615	0.4608	0.4600	0.4640	0.4614	0.4632
C2	-0.2799	-0.2779	-0.2783	-0.2868	-0.2871	-0.2846
N6	-0.4704	-0.4709	-0.4716	-0.4687	-0.4704	-0.4702
S8	0.3670	0.3748	0.3674	0.3916	0.3798	0.3798
C9	-0.3229	-0.2650	-0.2674	-0.2540	-0.2679	-0.2642
C10	0.6895	0.6862	0.6859	0.6874	0.6812	0.6861
O23	-0.5987	-0.6115	-0.6148	-0.5997	-0.6064	-0.6066
N24	-0.7674	-0.7676	-0.7686	-0.7633	-0.7651	-0.7651
N29	-0.3424	-0.3459	-0.3476	-0.3329	-0.3391	-0.3397
N30	-0.3007	-0.3038	-0.3077	-0.2853	-0.2966	-0.2976
C40	0.2775	0.2779	0.2786	0.2726	0.2739	0.2752
O37	--------	--------	-0.5218	-0.3759	--------	--------
O46	--------	--------	-0.5110	-0.3763	--------	--------
N41	--------	--------	--------	-0.5136	--------	--------
N42	--------	--------	--------	-0.0853	--------	--------
O44	---------	---------	---------	-0.1440	---------	---------
O45	--------	--------	--------	-0.1438	--------	--------
Cl41	--------	--------	--------	--------	0.0142	------
Cl42	--------	--------	--------	--------	0.0060	-------
Br41	---------	---------	---------	-------	-------	0.0806
Br42	--------	--------	--------	--------	--------	0.0606

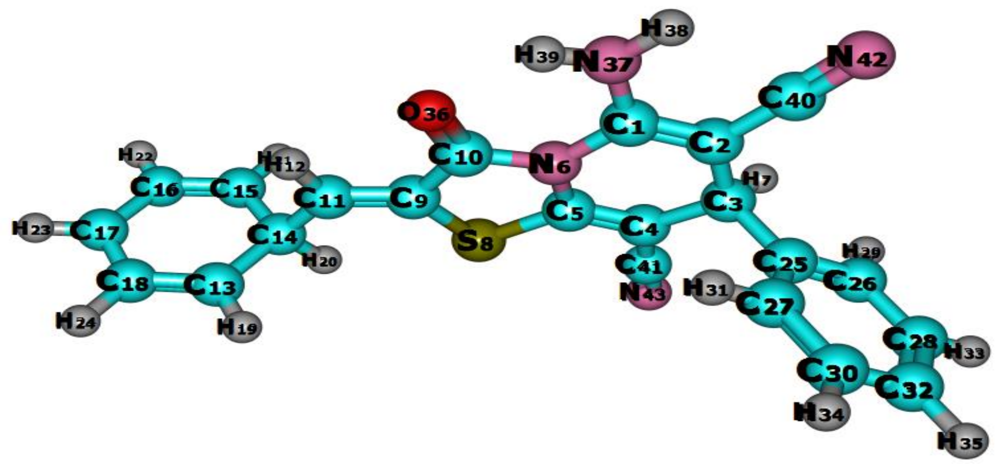

23

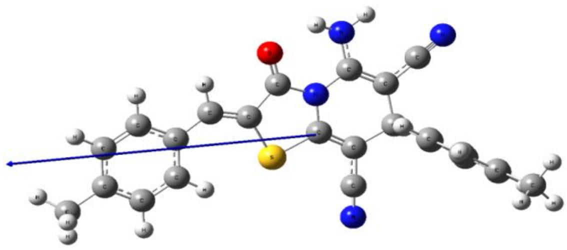

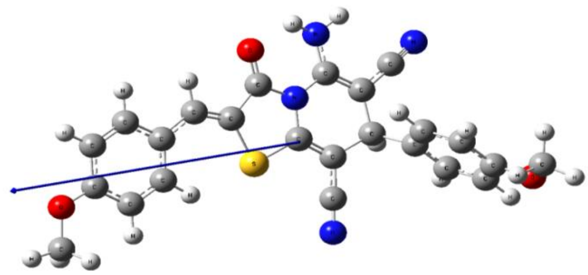

24 **25**

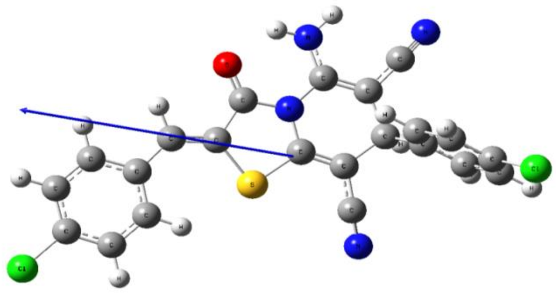

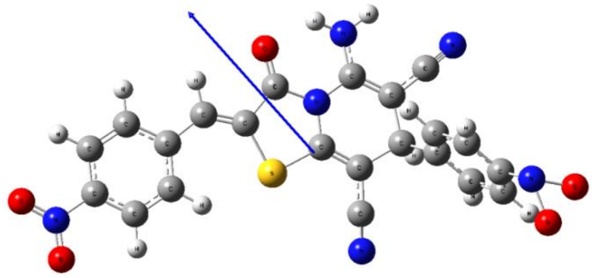

26 **27**

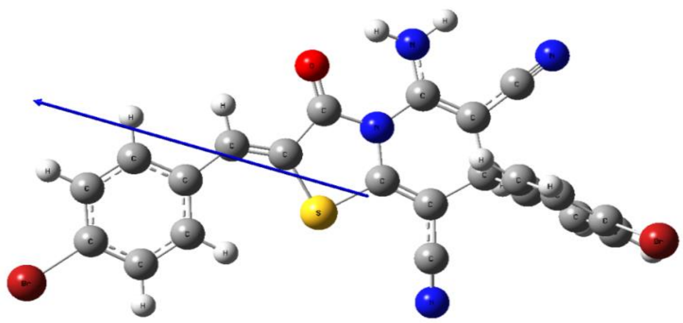

28

Fig. 3. Optimized geometry, vector of the dipole moment and numbering system, for the studied compounds **23-28** at B3LYP/6-311G (d, p).

3.3. Global reactivity descriptors

They include HOMO, LUMO, energy gap (E_g), chemical hardness (η), electronegativity (X), chemical potential (V), electrophilicity (ω), electron affinity (A), ionization potential (I) and global softness(S) which are calculated at B3LYP/6-311G (d,p) .The frontier molecular orbital (FMO) energies of the studied compounds were calculated at the same level of theory. HOMO energy characterizes the electron donating ability, while LUMO energy characterizes the electron withdrawing ability. Energy gap (E_g) between HOMO and LUMO characterizes the molecular chemical stability which is a critical parameter in determining molecular electrical transport properties because it is a measure of electron conductivity. The results in Figure 4 and Table 6 indicate that the smaller the energy gap the easier the charge transfer and the polarization occurs within the molecule. Furthermore, the order of increasing reactivity in the studied compounds is: **26** >> **28** > **27** > **24** > **25** > **23**. The insignificant differences in E_g of all the studied compounds except **26** is due to the non-planarity of the two ph-X and ph-Y with the thiazolo[3,2-a]pyridine moiety (c.f. Table 6). Using HOMO and LUMO energies, ionization potential and electron affinity can be expressed as I~ -E_{HOMO}, A~ -E_{LUMO} at the B3LYP/6-311G (d,p) as shown in (Table 6). The variation of electronegativity (X) values is supported by electrostatic potential, for any two molecules, where electron will be partially transferred from one of low X to that of high X. The results show that the order of decreasing X is: **24** < **25** < **23** < **26** < **28** < **27**. The chemical hardness (η) = (I-A)/2, electronegativity(X) = (I+A)/2, chemical potential (V) = - (I+A)/2, electrophilicity (ω)=μ^2/ 2$\eta$and global softness(S) =1/2η values are calculated and presented in Table 6. The results of small η values for the studied compounds reflect the ability of charge transfer inside the molecule. Therefore, the order is: **26** > **28** > **27** > **24** > **25** > **23**. There is a linear relationship between η and E_g as shown in (Table 6).Considering η values, the higher the η values, the harder is the molecule and vice versa.

Table 6. Total energy, energy of HOMO and LUMO, energy gap , dipole moment, The ionization potential (**I** /eV), electron affinity (**A** /eV), chemical hardness (***η*** / eV), global softness (**S**/ eV^{-1}), chemical potential (***V/eV^{-1}***), electronegativity (***χ*** /eV), and global electrophilicity index, (***ω***/eV), of the studied compounds (**23-28**) computed at the B3LYP/6-311G(d,P)

Compounds	**23**	**24**	**25**	**26**	**27**	**28**
E_T (au)	-1539.9973	-1618.1178	-1768.5711	-1948.4386	-2458.7031	-6686.5442
E_{HOMO} (eV)	-6.28021	-6.12734	-6.01691	-6.68957	-6.41757	-6.40152
E_{LUMO} (eV)	-2.82499	-2.81030	-2.69090	-3.75197	-3.15275	-3.14949
E_{gap} (eV)	3.45522	3.31704	3.32602	2.93761	3.26482	3.25203
μ (Debye)	6.17941	7.32921	8.41721	5.82951	6.48671	6.48501
***I** (eV)*	6.28021	6.12734	6.01691	6.68957	6.41757	6.40152
***A**(eV)*	2.82499	2.81030	2.69090	3.75197	3.15275	3.14949
***X**(eV)*	4.55261	4.46881	4.35391	5.22081	4.78521	4.77551
***V**(eV^{-1})*	-4.55261	-4.46881	-4.35391	-5.22081	-4.78521	-4.77551
***η**(eV)*	1.72761	1.65851	1.66301	1.46881	1.63241	1.62601
***S**(eV^{-1})*	0.28942	0.30147	0.30066	0.34041	0.30629	0.30750
ω (eV)	5.99851	6.02061	5.69951	9.27861	7.01361	7.01271

23	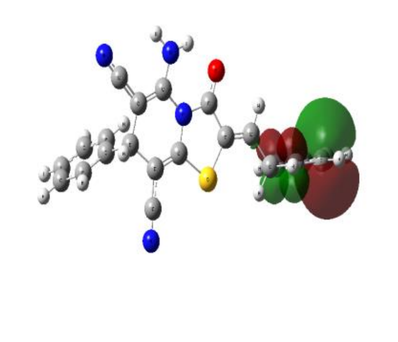	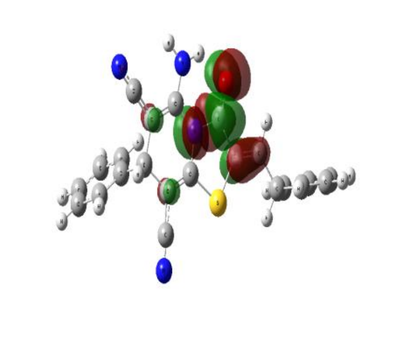	LUMO plot (first excited state) E_{LUMO} = -2.8250eV Egap = 3.4552eV E_{HOMO} = -6.2802eV HOMO plot (ground state)
	HOMO	LUMO	HOMO and LUMO energy band gap
25	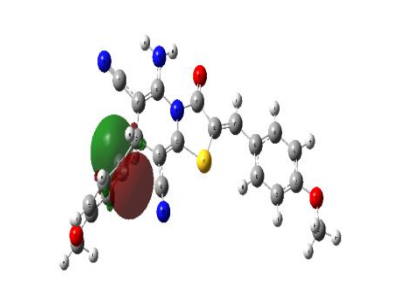	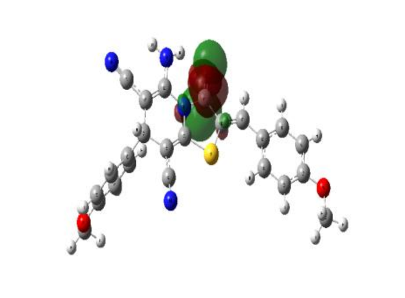	LUMO plot (first excited state) E_{LUMO} = -2.6909eV Egap = 3.3260eV E_{HOMO} = -6.0169eV HOMO plot (ground state)
	HOMO	LUMO	HOMO and LUMO energy band gap
26	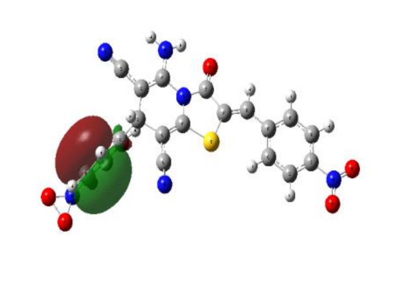	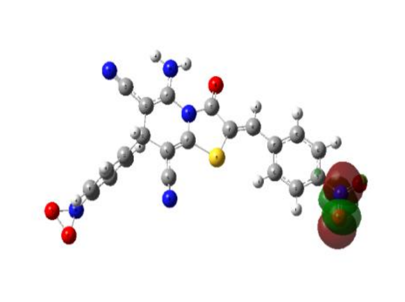	LUMO plot (first excited state) E_{LUMO} = -3.7520eV Egap = 2.9376eV E_{HOMO} = -6.6896eV HOMO plot (ground state)
	HOMO	LUMO	HOMO and LUMO energy band gap
3DMEP	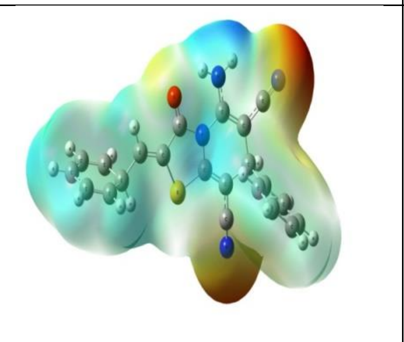	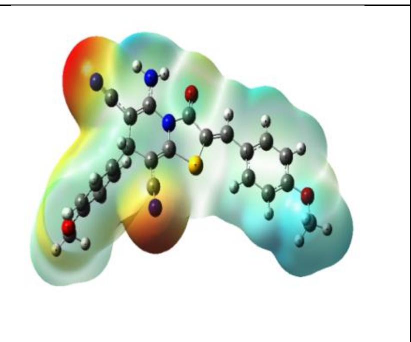	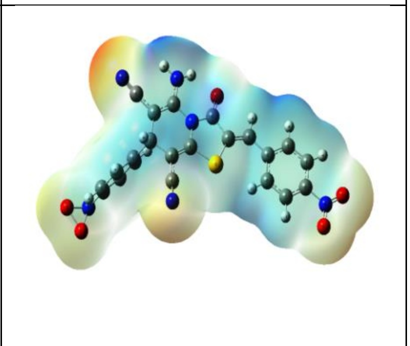
	23	**25**	**26**

Fig.4. HOMO and LUMO maps, energy gap and 3D MEP of **23, 25** and **26** at B3LYP/6-311G (d, p).

The color scheme for the MEP surface is as follows: red for electron rich, (partially negative charge); blue for electron deficient,(partially positive charge); light blue for (slightly electron deficient region); yellow for (slightly electron rich region); green for neutral (zero potential) respectively.

3.4. Nonlinear optical (NLO) Analysis

So far no experimental or theoretical investigations were found addressing NLO for these classes of molecules; therefore, this triggered our interest to undertake this study. NLO is at the forefront of current research due to its importance in providing key functions of frequency shifting, optical modulation, switching , laser, fiber, optical materials logic and optical memory for the emerging technologies in areas such as telecommunications, signal processing and optical inter connections [35]. In order to investigate the relationship between molecular structure and NLO, the polarizibilities and hyperpolarizibilities of the studied compounds **23-28** are calculated using DFT/B3LYP/6-311G (d,p). Total static dipole moment (μ), the mean polarizibility α, the anisotropy of the polarizability Δα, the mean first-order hyperpolarizibility (β) of the studied compounds **23-28** are listed in Table 7.

The polarizibilities, and first-order hyperpolarizibilities are reported in atomic units (a.u.), the calculated values have been converted into electrostatic units (esu) using conversion factor of 0.1482×10^{-24}esu for α and 8.6393×10^{-30}esu for β. P-nitro aniline (PNA) is a standard prototype used in NLO studies. In this study, PNA is chosen as a reference as there were no experimental values of NLO properties of the studied compounds. The values of α, β in Table 7 show that the order of increasing αwith respect to PNA is: compounds **28** and **25**are ~ 3 times higher than (PNA), compounds **27** and **24** are ~ 2.5times higher than the standard, whereas compounds **23** and **26** are ~ 2 and1.5times higher than (PNA) respectively, The calculated first order hyperpolarizability of p- nitroacetanilide (PNA) is 15.482×10^{-30}esu as reported by T. Gnanasamb and et al [36-38]. The analysis of the β parameter show that compounds **24** and **25** are ~ 2 and 2.5 times higher than (PNA), while compounds **28**, **23**, **27** and**26** are~ 1.8, 1.3, 1.2 and 0.7times higher than the referencerespectively.

Table 7. Total static dipol moment (**μ**), the mean polarizability (<**α**>), the anisotropy of the polarizability (**Δα**), and the mean first-order hyperpolarizability (<**β**>), for the studied compounds (**23-28**) computed at B3LYP/6-311G(d,P)

Property	PNA	23	24	25	26	27	28
μ_x, D		-2.24430	2.61289	2.85246	1.35945	2.32008	2.30742
μ_y, D		0.08666	-0.24590	-0.88641	1.73073	0.72274	0.49933
μ_z, D		0.93070	-1.18942	- 1.42621	-0.66068	-0.7736	-0.9645
μ, Debye [a]	2.44	2.43117	2.88139	3.31004	2.29783	2.55020	2.55027
α_{XX}, a.u.		482.413	587.615	598.724	-269.80	595.423	623.326
α_{XY}, a.u.		-30.944	-0.1592	-15.607	19.293	-5.7605	-22.507
α_{YY}, a.u.		239.479	293.091	302.815	-220.57	288.783	289.420
α_{ZZ}, a.u.		-28.470	-41.650	-43.762	-201.81	-44.285	-54.675
α_{YZ}, a.u.		6.79178	-30.350	-38.402	-2.5460	-36.345	-39.028
α_{XZ}, a.u.		211.708	211.621	236.477	-9.1518	210.854	233.861
<**α**> $\times10^{-24}$ esu [b]	22	46.12	53.96	56.22	34.19	54.24	56.64
Δα $\times10^{-24}$ esu		39.76	52.47	51.87	10.57	54.10	57.05
βxxx, a.u.		-220.85	-345.36	387.720	-125.60	209.479	264.923
βxxy, a.u.		-119.74	-179.07	-256.94	164.153	-27.898	-109.09
βxyy, a.u.		-50.136	-73.659	119.433	82.180	94.2996	112.768
βyyy, a.u.		55.4519	25.0538	-45.685	13.983	12.7179	-159.59
βxxz, a.u.		22.8061	49.3277	-32.884	36.707	5.8558	-8.5066

Table 7. Continued

βxyz, a.u.		6.8009	-15.274	-59.051	32.432	3.0237	-17.415
βyyz, a.u.		47.3040	48.8812	-60.547	-36.802	-35.854	-47.901
βxzz, a.u.		-6.9762	19.7439	-42.837	7.6480	-5.6797	10.645
βyzz, a.u.		11.2137	17.5866	0.0221	16.082	22.7894	-18.436
βzzz, a.u.		31.6823	30.8810	-61.499	-35.323	-38.325	-81.666
$\langle\beta\rangle \times 10^{-30}$ esu[c]	15.5	19.862	30.034	34.144	11.337	18.431	27.635

a, b, c PNA results are taken from references [36–38].

3.5. Molecular electrostatic potential (MEP)

Molecular electrostatic potential (MEP) is related to the electronicdensity and is a very useful descriptor in understanding sitesfor electrophilic and nucleophilic attack as well as hydrogenbonding interactions [39].This is correlated with dipole moments,electro negativity, partial chargesand chemical reactivityof the molecules. These maps allow us to visualize variably chargedregions of a molecule. Knowledge of the charge distributions can be used to determine how molecules interact with one another. The calculated 3D MEP of some selected molecules (**23, 25** and **26**) are calculated from optimized molecular structure using DFT/B3LYP/6-311G (d,p)are shown in Figure 4. The results show that , in case of **23**(X=Y=H) the negative region (red) is mainly over the Nand O atomic sites, which is caused by the contribution of lone-pair electrons of nitrogen andoxygen atoms while the positive (blue) potential sites are around the hydrogen,sulfur and carbon atoms. A portion of the molecule that has negative electrostatic potential will be susceptible to electrophilic attack—the more negative the higher the tendency for electrophilic attack. The color scheme for the MEP surface is as follows: red for electron rich, (partially negative charge); blue for electron deficient,(partially positive charge); light blue for (slightly electron deficient region); yellow for (slightly electron rich region); green for neutral (zero potential) respectively. Potential increases in the following order: red < orange < yellow < green < blue [40, 41].

3.6. Biological activity

The biological activity of the studied compounds **(23-28)** was tested against Grame positive bacteria, Grame negative bacteria with Ampicillin and Fungi with Mycostatine as standard reference for each respectively as shown in Table 8 and Figures (6-8). Concerning Grame positive bacteria, two types of bacteria were used in the testing procedure, which are S.aureus and B.cereus. The parent compound **23** was less to moderatebiologically active compared to standard reference, while the substituted compounds showed different biological activity. Compound **24** was moderately active compared to the parent and the substituted compounds (**25, 26, 27** and **28**) were highly active than the parent compound **23**. Concerning Grame negative bacteria, two types of bacteria were also used in the testing procedure, which are S.marcesens and P.mirabilis. The parent compound **23** showed less to moderate biological activity compared to standard reference. On the other hand, the substituted compounds showed variations in the biological response, Compound **24** was highly active compared to the parent compound **23,** while the substituted compounds (**25, 26, 27** and **28**) were moderately active compared to the parent. Moving to Fungi, A.ochraceus Wilhelm and P.chrysogenum Thom were the two types used in the testing procedure. The parent compound **23** showed less to moderate biological activity compared to standard reference. All the substituted compounds (**24, 25, 26, 27** and **28**) showed moderate in the biological activity compared to the parent.

The studied compounds can be arranged according to their biological activity against Grame positive bacteria, Grame negative bacteria and Fungi compared to standard reference as follows: Compound **26,** comes first with the highest biological activity, than compound **28**, this is followed by **27, 25, 24** and the parent compound **23,** is the last one with the least biological activity i.e. **26** > **28** > **27** > **24** > **25** > **23.**

Table 8. Antimicrobial Activity for the studied compounds **23-28**

Compounds	**Inhibition zone (mm) at conc. of (µg/ml)**					
	Grame positive bacteria		**Grame negative bacteria**		**Fungi**	
	S.aureus	**B.cereus**	**S.marcesens**	**P.mirabilis**	**A.ochraceus Wilhelm**	**P.chrysogenum Thom**
23	1	0.35	1	0.35	1	0.35
24	1	0.35	2.25	0.35	0.35	1
25	2.25	0.35	1	0.35	1	0.35
26	2.25	1	1	2.25	1	1
27	2.25	1	1	1	1	0.35
28	2.25	1	1	1	0.35	1
Standard	3	3	2.25	2.25	3	3

0.35: Less active (0.2-0.5 cm)
1: Moderately active (0.6-1.4 cm)
2.25: Highly active (1.5-3.0 cm)
3: Very highly activity (over 3.0 cm)

Standard: For Grame positive bacteria and Grame negative bacteria: Ampicillin 25 µg/ml; for fungi: Mycostatine 30 µg/ml.

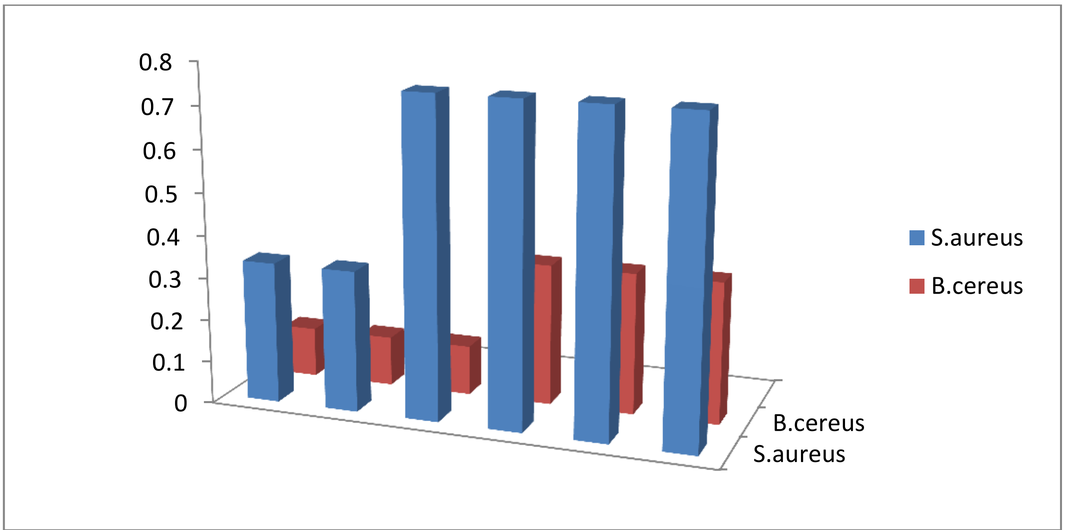

Fig.6. Biological activity for the studied compounds **23-28** against gram-positive bacteria (G^+).

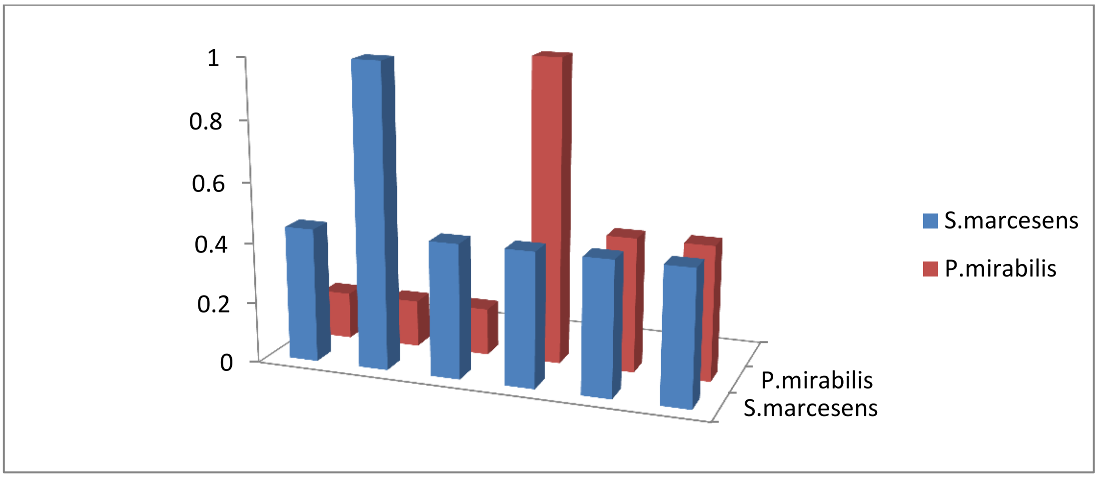

Fig.7. Biological activity for the studied compounds **23-28** against gram-negative bacteria (G^-).

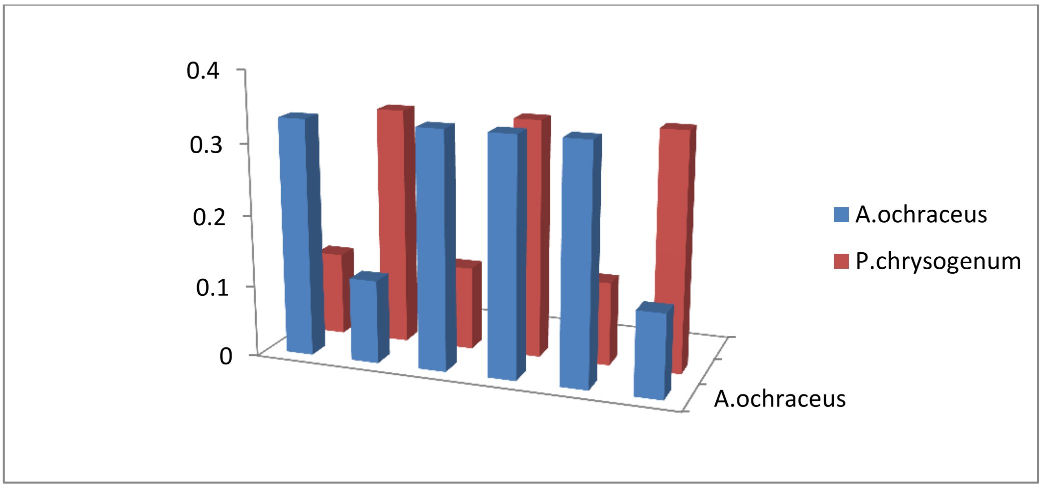

Fig. 8. Biological activity for the studied compounds **23-28** against Fungi.

3.7. Correlation between biological and ground state properties

The biological activity of the studied compounds can be correlated with the ground state energetic and global properties. From the computed data in (Table 6), one can reveal the following: The biological activity of the studied compound obtained experimentally follow the order **26** > **28** > **27** > **24** > **25** > **23**, Against G+, G- and fungi. The theoretical chemical reactivity, Eg, of the studied compound computed at B3LYP/6-311G (d,p) follow the same order obtained experimentally indicating that Eg is one factor contributing to the reactivity of the studied compounds (c.f. Table 6). The theoretically computed global softness (S) and natural charge from NBO of the studied compounds follow the same order of the experimental biological activity which is **26** > **28** > **27** > **24** > **25** > **23**. Whereas, the chemical hardness (η) follow the reverse order of the experimental biological activity **23** > **25** > **24** > **27** > **28** > **26.** In case of electronegativity (χ), global electrophilicity index, (ω), chemical potential (V) and mean first-order hyperpolarizability (β), the order are **26** > **27** > **28** > **23** > **24** > **25** which violate the order of the experimental biological activity.

4- CONCLUSION

The molecular geometry of poly-functions thaizolo [3,2-a] pyridine derivatives in the ground state has been calculated by using DFT-B3LYP/6-311G (d,p) level of theory. The optimized structure of the studied compounds **23-28** are non-planner with the two phenyl at C_3 and C_9 are out of the molecular plane of thaizolo [3, 2-a] pyridine with a dihedral angles of 71.5^o and 116.4^o respectively. From the artificial partitioning of the parent compound **23**, it is clear that the subsystem **12** is responsible for the stability, donating property, energy gap and polarity of the parent molecule **23**. The small difference between E_g of the studied compounds **23-28** may be attributed to the presence of the two Ph-x and Ph-y out of the molecular plane of thaizolo [3, 2-a] pyridine moiety. The HOMO-LUMO energy gap helped in analyzing the chemical reactivity, hardness, softness, chemical potential and electro negativity. Mullikan and natural charge distribution of the molecule were studied which indicated the electronic charge distribution in the molecule. The calculated dipole moment and first order hyperpolarizability results indicate that the molecule has a reasonable good non-linear optical behavior. The NBO analysis indicated the intermolecular charge transfer between the bonding and antibonding orbital's. MEP confirmed the different negative and positive potential sites of the some selected molecules in accordance with the total electron density surface. The biological activity of the studied compounds show that compound **26** (**NO_2**) is the most active one, whereas, the parent molecule **23** (**H**) is the least active and the order of reactivity is **26 > 28 > 27 > 24 > 25 > 23.**

Conflicts of interest: The Manuscript that do not include a conflict of interest, and so there is no funded entity for this research**.**

REFERENCES

[1] M. Khalifa NagyAdel, A.H. Abdel-Rahman, A. Abd ElGwaadAmina, A. Al-Omar Mohamed Asian, J. Chem. 26 (2014) 8202.

[2] S. Vadivelan, B. Sinha, N. Irudayam, S. J. Jagarlapudi, S.A.R.P, J. Chem. Inf. Model. 47(2007)1526.

[3] H. Park, K. Hwang, Y. Oh, K. H.; Kim, Y. H.; Lee, J. Y.; Kim, K, Bioorg. Med. Chem. 16 (2008) 476-84.

[4] Shi. Feng, Li.Chunmei, Xia. Ming, Miao. Kangjie, Zhao. Yanxia, Tu. Shujiang, WeifaZheng, Ge. Zhang, Ma. Ning, Green chemoselective, Bioorg. and Med. Chem. Lett. 19 (2009) 5565.

[5] A. R. Sreekanth, Vijay Nair, N. Abhilash, M. Bhadbhade Mohan, C. Gonnade Rajesh, Org. Lett. 4 (2002) 3575.

[6] (a) G. El-Hag Ali, Khalil, A. Lamphon, R.; El-Maghraby, A. Phosphorus. Sulfur. Silicon Relate. Elem. 180 (2005) 1909. (b) A. El-Maghraby, A.; El-Hag Ali, G.A.M., Ahmed, A.H.A.; El-Gaby, M.S.A. Phosphorus, Sulfur Silicon Relate. Elem. 177 (2002) 293.

[7] El-Gaby, M.; Al-Sehemi, A.; Mohamed, Y.; Ammar, Y., Phosphorus. Sulfur and Silicon and the Related Elements. 181 (2006) 631.

[8] (a) J. Valenciano, E. Sa´nchez-Pavo´n, A. Cuadro, M. Vaquero, J. J. Alvarez-Builla, J. J. Org. Chem. 66 (2001) 8528. (b) A. Dombrowski, M. Nieger, E. Niecke, Chem. Commun. (1996) 1705. (c) K. Potts, T. Rochanapruk, T. Coats, S. J. Hadjiarapoglou, L. Padwa, A. J. Org. Chem. 58 (1993) 5040. (d) K. Potts, T. Dery, M. O. J. Org. Chem. 55

(1990) 2884. (e) H. Gotthardt, M. Riegels, Chem. Ber. 121 (1988) 1143. (f) I. Ungureanu, P. Klotz, A. Shoenfelder, A. Mann, Chem. Commun. (2001) 958. (g) J. Rigby, H. Synlett, (2000) 1. (h) J. Tejeda, R.Reau, F. Dahan, G. Bertrand, J. Am. Chem. Soc. 115 (1993) 7880. (i) T. Facklam, O. Wagner, H. Heydt, M. Regitz, Angew. Chem.Int. Ed. Engl. 29 (1990) 314.

[9] (a) V. Nair, R. Menon, S. Sreekanth, A. R. Abhilash, N. Biju, A. T. Acc. Chem. Res. 39 (2006) 520. (b) V. Nair, A. Sreekanth, R. Abhilash, N. Bhadbhade, M. M. Gonnade, R. C. Org. Lett. 4 (2002) 3575. (c) V. Nair, A. Sreekanth, R. Biju, A. T. Rath, N. P. Tetrahedron Lett. 44 (2003) 729.

[10] G. A. M. El-Hag Ali, A. Khalil, A. H. A. Ahmed, M. S. A. El-Gaby, Acta. Chim. Slov. 49 (2002) 365.

[11] K. Mandal, T. Kar, P.K. Nandi, S.P. Bhattacharyya, Chem. Phys. Lett. 376 (2003) 116.

[12] P. K. Nandi, K. Mandal, T. Kar, Chem. Phys. Lett. 381 (2003) 230.

[13] P. N. Prasad, D. J. Williams, John Wiley & Sons, New York, NY, USA (1991).

[14] F. Meyers, S. R. Marder, B. M. Pierce, J.L. Brédas, J. Amer. Chem. Soc. 116 (1994) 10703.

[15] J. P. Foster and F. Weinhold, J. Amer. Chem. Soc. 102 (1980) 7211.

[16] A. E. Reed, L. A. Curtiss, F. Weinhold, Chem. Rev. 88 (1988) 899.

[17] S. Abdel Halim, Ali Kh. Khalil J. Mol. Struct. 1147 (2017) 651.

[18] (a) A. D. Becke, J. Chem. Phys. 98 (1993) 5648 (b) A. D. Becke, J. Chem. Phys. 98 (1993) 1372.

[19] (a) C. Lee, W. Yang, R.G. Parr, Phys. Rev. BCondens. Matter. 37 (1988) 785 (b) B. Miehlich, A. Savin, H. Stolt, H. Preuss, Chem. Phys. Lett. 157 (1989) 200.

[20] B. Stefanov, B. G. Liu, A. Liashenko, P. Piskorz, I. Komaromi, R.L. Martin, D.J. Fox, T. Keith, M.A. Al-Laham, C.Y. Peng, A. Nanayakkara, M. Challacombe, P.M. W. Gill, B. Johnson, W. Chen, M.W. Wong, C. Gonzalez, J.A. Pople, Gaussian, Inc., Pittsburgh PA. (2003).

[21] M. Frisch, J.G.W. Trucks, H.B. Schlegel, G.E. Scuseria, et al., Gaussian, Inc., Wallingford CT, (2009).

[22] GaussView, Version 5, Dennington, R.; Keith, T.; Millam, J. Semichem Inc., Shawnee Mission KS, (2009).

[23] http://www.chemcraftprog.com.

[24] D. Avci, Spectrochim.Acta A. 82 (2011) 37.

[25] D. Avci, A. Başoğlu, Y. Atalay, Struct. Chem. 21 (2010) 213.

[26] D. Avci, H. Cömert, Y. Atalay, J. Mol. Mod. 14 (2008) 161.

[27] R. G. Pearson, Proc. Nat. Acad. Sci. 83 (1986) 8440.

[28] A. K. Chandra and T. Uchimara, J. Phys. Chem. A. 105 (2001) 3578.

[29] J. Chocholoušová, V. Špirko, and P. Hobza, J. Phys. Chem. Chem. Phys. 6 (2004) 37.

[30] M. Szafran, A. Komasa, E. Bartoszak-Adamska, J. Mol. Struct. 827 (2007) 101.

[31] A. Gamal El-Hiti, Keith Smith, Amany S. Hegazy, Ali M. Masmali and Benson M. Kariuki, Acta. Cryst. E70 (2014) 0932.

[32] A. Gamal El-Hiti, Keith Smith, Amany S. Hegazy, Saud A. Alanazi, Benson M. Kariuki, Acta. Cryst. E71 (2015) 0562.

[33] A. Gamal El-Hiti, Keith Smith, Amany S. Hegazy, Mansour D. Ajarim, Benson M. Kariuki, Acta. Cryst. E71 (2015) 0877.

[34] M. Snehalatha, C. Ravikumar, I. Hubert Joe, N. Sekar, V.S. Jayakumar, Spectrochim. Acta. 72A. (2009) 654.

[35] S. Natorajan, G. Shanmugam and S. A. MartinCryst. Res. Technal. 43 (2008) 561; D.S. Chemia, J. Zysss, Academic Press, Orlando, FL, (1987) D. S. Bradshow, D. L. Andrews, J. Nonlinear Opt. Phys. Matter. 18 (2009) 285.

[36] L.T. Cheng, W. Tam, S. H. Stevenson, G. R. Meredith, G. Rikken, S. R. Marder, J. Phys. Chem., 95 (1991) 10631.

[37] [P. Kaatz, E. A. Donley, D. P. Shelton, J. Chem. Phys., 108 (1998) 849.

.

[38] [T. Gnanasambandan, S. Gunasekaran, S. Seshadri, Spectrochimica. Acta Part A: Molecular and Biomolecular Spectroscopy. 117 (2014) 557.

[39] J. S. Murray, K. Sen, Elsevier, Amsterdam, (1996) 7 and E. Sscrocco, J. Tomasi, Adv. Quant. Chem. 11 (1978) 115.

[40] P. Politzer, J.S. Murray, Theor. Chem. Acc. 108 (2002) 134.

[41] D. Sajan, L. Joseph, N. Vijayan, M. Karabacak, Spectrochim. Acta. A. 81(2011) 85.